EXACERBATED HEMOLYTIC ANEMIA WITH EXPOSURE TO PHENYLHYDRAZINE IN HRI DEFICIENCY

Sijin Liu[1,2], Rajasekhar N.V.S. Suragani[2], and Jane-Jane Chen[2]

1. Research Center for Eco-Environmental Sciences, Chinese Academy of Sciences, Beijing 100085, China.
2. Harvard-MIT Division of Health Sciences and Technology, Massachusetts Institute of Technology, Cambridge, Massachusetts, USA.

Abstract

Phenylhydrazine (PHZ) exposure may cause adverse health issues via inhalation, ingestion, or dermal or eye contact. PHZ has been documented to cause severe hemolytic anemia, degenerative lesions in livers and kidneys and lung tumors in animals or humans. Heme-regulated eIF2α kinase (HRI) plays an essential protective role in anemias of iron deficiency, erythroid protoporphyria, and β-thalassemia. The current study indicates that HRI is important for macrophage maturation, although it is expressed at a lower level in macrophages. In HRI deficiency, macrophages do not develop the typical morphology and expressed less CSF-1R protein. Consequently, expression levels of macrophage cell-surface markers F4/80 and CD11b and the core component of the receptor complex for LPS, TLR4, are reduced in $Hri^{-/-}$ compared with $Hri^{+/+}$ macrophages. This is the first demonstration that HRI protein is expressed and functional in nonerythroid cell types. Further, an impairment of erythrophagocytosis by $Hri^{-/-}$ macrophages was observed under chronic hemolytic anemia induced by PHZ in vivo, providing evidence for the role of HRI in recycling iron from senescent red blood cells. This work demonstrates that HRI deficiency attenuates iron homeostasis in mice, indicating a protective role for HRI in hemolytic anemia of inflammation with exposure to PHZ.

Introduction

Phenylhydrazine (PHZ) and its derivatives, as a family of aromatic amines, are widely used intermediates for manufacture of pesticides and dyestuffs. These compounds have been demonstrated to induce hemolytic anemia, hepatic and renal damages, and lung tumors. PHZ can enter the environment through industrial discharges or through spills. Because of their high toxicity and poor biodegradability, they have become an environmental concern. The impairment to red blood cells (RBCs) by PHZ is due to its haemolytic action. PHZ leads to increased level of H_20_2 within RBCs, and also causes oxidative alterations to the integrity of blood cell membrane.

Heme-regulated eIF2α kinase (HRI) is expressed mainly in erythroid cells and is an important physiological regulator of gene expression and cell survival in the erythroid lineage. HRI plays essential protective roles in iron deficiency [1], erythropoietic protoporphyria (EPP), and β-thalassemia [2]. HRI exerts these functions in part by controlling protein synthesis via phosphorylation of the α-subunit of the eukaryotic translational initiation factor 2 (eIF2α). HRI normally insures that no globin is synthesized in excess of what can be assembled into hemoglobin tetramers, which is dependent on the amount of heme available. HRI is also activated by non-heme cytoplasmic stresses such as oxidative stress induced by arsenite [3].

Systemic iron homeostasis is strictly regulated to supply the appropriate amount of iron for growth and survival while preventing either iron deficiency or iron excess. The liver-produced hormone hepcidin is the key regulator in this dynamic process. Hepcidin controls plasma iron levels by inhibiting the absorption of dietary iron from the intestine and the release of iron from senescent RBCs by macrophages. Hepcidin exerts this function by binding to the iron exporter ferroportin and targeting ferroportin for degradation [4].

In the current paper, a novel function of HRI in macrophages is reported. Expression of HRI is necessary for the maturation of macrophages. When treated by PHZ, $Hri^{-/-}$ mice display chronic

hemolytic anemia with diminished iron recycling. This study demonstrates the function of HRI in iron homeostasis and indicates that HRI may be important in hemolytic anemia induced by PHZ.

Materials and Methods

Mouse strains, breeding, and genotyping. $Hri^{-/-}$ mice on an inbred B6.129 mixed genetic background were generated as described previously [1]. Genotyping was performed by PCR of tail DNA. PCR reactions of the Hri gene were performed as described previously [1].

Non-heme iron assays. Blood, liver, and spleen samples were collected from 4-month-old mice. Non-heme tissue iron was assayed as previously described [5].

qRT-PCR. Total RNAs were isolated from liver tissues using Total RNA Isolation kit (Promega). Quantitative measurements of gene expression were carried out with DNA Engine Opticon 2 (MJ Research) equipped with Opticon Monitor 2 software. eIF2α was used as an internal control. Primer sequences were hepcidin: forward 5′-CTGAGCAGCACCACCTATCTC-3′, reverse 5′-TGGCTCTAGGCTATGTTTTGC-3′; eIF2α: forward 5′-GGAAGCAATCAAATG-TGAGGA-CA-3′, reverse: 5′-GCACCGTATCCAGGTCTCTTG-3′.

Cell culture of BMDMs. Bone marrow–derived macrophages (BMDMs) were isolated and cultured as previously described [6]. Briefly, bone marrow cells were flushed from the femur and tibia of 6- to 8-week-old male mice, washed twice with PBS plus 2% FBS, and then cultured in DMEM with high glucose, glutamine, 15% heat-inactivated FBS, 25 ng/ml rmCSF-1 (PeproTech), nonessential amino acids (Cambrex), penicillin/streptomycin (Invitrogen), and 55 nM β-ME (Sigma-Aldrich) at 37°C, 5% CO2. Three days after seeding, cells were washed twice with PBS, and the medium was changed every day until day 7.

Immunofluorescence microscopy. Immunofluorescence study was done according to the standard procedures. BMDMs were cultured on coverslips as described above and were fixed in 4% paraformaldehyde for 15 minutes at 37°C. After washing 3 times with PBS, cells were permeabilized with 0.1% Triton X-100 in PBS for 10 minutes at room temperature. Cells were blocked for 2 hours with PBS plus 5% normal goat serum and 1% BSA. Cells were incubated overnight at 4°C with 1:500 anti-HRI IgG and 1:10 anti-CD11b (Mac-1) antibody (BD Biosciences). Cells were then washed 5 times with PBS followed by incubation for 90 min with the anti-rabbit (for HRI) or anti-rat (for Mac-1) IgG secondary antibody conjugated with Alexa Fluor 488 or Alexa Fluor 633 (Molecular Probes; Invitrogen). After washing with PBS, coverslips were air dried and then mounted with anti-fading mounting reagent and examined by an LSM 410 inverted laser scan microscope (LSM Technologies Inc.).

Flow cytometry. Expression of CD11b, F4/80, and TLR4 in bone marrow cells and BMDMs were examined by flow cytometry. Cultured BMDMs were detached from the culture dishes on days 3 and 6 by treatment with 5 mM EDTA for 15 minutes. Both bone marrow cells and BMDMs were washed twice with PBS and then stained with allophycocyanin-conjugated rat anti-mouse CD11b monoclonal antibody (BD Biosciences), or FITC-conjugated rat anti-mouse F4/80 monoclonal antibody (eBioscience) for 30 minutes on ice. After washing 3 times with PBS, cells were analyzed by flow cytometry as described previously [1].

Western blot analysis. Protein extracts were prepared from macrophages as previously described [1]. Protein extracts (20 μg) were separated SDS-PAGE and processed for Western blot analyses as described previously [1]. Antibodies used were the affinity-purified anti-mouse N-terminal HRI antibody (1:1,000), anti-eIF2αP antibody (1:1,000; BioSource), anti–CSF-1R (1:500; Santa Cruz Biotechnology Inc.) or anti-eIF2α antibody (1:1,000; BioSource). The intensities of western signals in autoradiograms were quantitated by Alpha Ease FC software (Alpha Innotech).

PHZ exposure in the mouse model. PHZ (Sigma-Aldrich), freshly prepared in PBS, was injected intraperitoneally into mice to exert a low-dose exposure. PHZ was given twice a week at a low dose (30 mg/kg) for 4 weeks, as previously used to induce chronic hemolytic anemia [7]. Mice were sacrificed at 64 hours after the final injection of PHZ, and blood, spleen, and liver samples were collected for complete blood count, iron, and hepcidin analyses.

Pathological analysis. Sections were stained with H&E. Liver and spleen non-heme iron were stained with Prussian blue as described previously [8].

Statistics. Statistical analyses among the various groups were performed by 2-tailed Student t test, with a P value of less than 0.05 considered statistically significant.

Results and Discussion

Expression of HRI in macrophages. Macrophages are pivotal constituents of the innate immune system, vital for recognition and elimination of microbial pathogens [9]. Macrophages are also responsible for iron recycling, taking iron from the hemoglobin of senescent RBCs by phagocytosis and releasing it to the serum through ferroportin [10, 11].

To investigate how HRI might regulate iron content in splenic macrophage and hepatic hepcidin expression, the expression of HRI in BMDMs cultured in vitro with CSF-1 was assessed. qRT-PCR analysis suggests that expression of HRI mRNA in BMDMs was approximately 2% of that in fetal liver erythroid precursors (data not shown). Expression of HRI protein in BMDMs was also demonstrated by immunofluorescence microscopy (Figure 1A) and Western blot analysis (Figure 1B). Most HRI-positive cells were Mac-1–positive macrophages, and HRI protein was located in the cytoplasm of macrophages (Figure 1A). Consistent with qRT-PCR results, HRI protein in BMDMs was also expressed at a lower level than that in fetal liver erythroid precursors (Figure 1B).

HRI is predominantly expressed in the erythroid lineage [12]. This is the first demonstration that HRI protein is expressed at a substantial level in nonerythroid cells. Most significantly, the level of phosphorylated eIF2α (eIF2αP) in Hri$^{-/-}$ BMDMs was diminished (about 50%) as compared with that in Hri+/+ BMDMs (Figure 1B). These results demonstrate that HRI is not only expressed in BMDMs but is also active and functional in phosphorylating its substrate, eIF2α. HRI contributes to 50% of the total eIF2α kinase activity in macrophages.

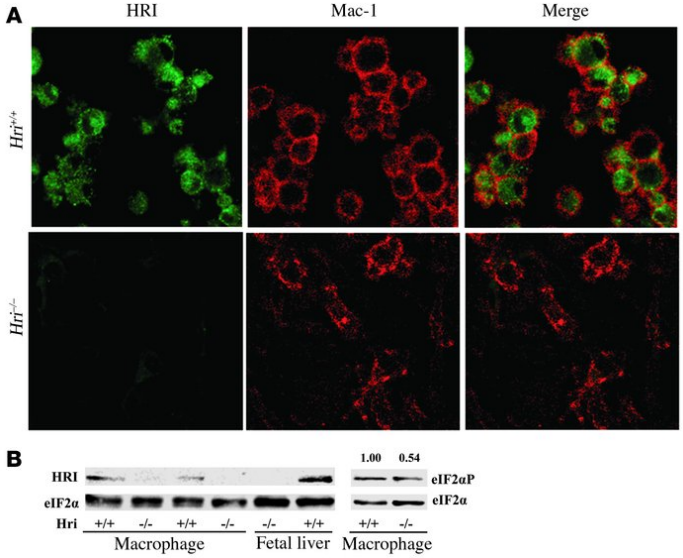

Figure 1. Expression of HRI protein in BMDMs. (A) Immunofluorescence staining of HRI and Mac-1 in *Hri*$^{+/+}$ and *Hri*$^{-/-}$ macrophages. Original magnification, ×400. (B) Western blot analyses of HRI protein, eIF2αP, and total eIF2α levels in *Hri*$^{+/+}$ and *Hri*$^{-/-}$ macrophages and E14.5 fetal liver cells. The intensities of autoradiograms were quantitated as described in Methods. The ratios of eIF2αP to eIF2α were calculated; the ratio in *Hri*$^{+/+}$ was defined as 1. The normalized ratios are shown above the autoradiogram.

Impairment of macrophage maturation in HRI deficiency. As shown by phase-contrast microscopy, BMDMs began to mature and form outward protrusions at the peripheral membrane in Hri$^{+/+}$ by day 3 of in vitro culture. In contrast, Hri$^{-/-}$ BMDMs were still round, without outward protrusions (Figure 2A). On day 6, most Hri$^{+/+}$ cells were typical macrophages; however, Hri$^{-/-}$ BMDMs were still less mature, with fewer podosomes, as shown in Figure 2A.

In vivo, the expression of CD11b (Mac-1) macrophage surface marker was 9.82% less in Hri$^{-/-}$ bone marrow cells than in Hri$^{+/+}$ bone marrow cells (day 0, $P < 0.05$; Figure 2B). After culturing bone marrow cells in vitro for 3 days with CSF-1, 96%–99% cells derived from both Hri$^{+/+}$ and Hri$^{-/-}$ bone marrow were F4/80- and CD11b-positive, with a significant increase in the expression levels of both macrophage surface markers. However, the expression levels of both CD11b and F4/80 in Hri$^{-/-}$ BMDMs were still lower than those in Hri$^{+/+}$ BMDMs on both day 3 and day 6 ($P < 0.05$; Figure 2B). As shown in Figure 3C, protein expression of TLR4, which plays an

important role in sensing LPS [13], was decreased by 42.5% ($P < 0.005$) in *Hri*$^{-/-}$ macrophages by FACS analysis. CSF-1 receptor (CSF-1R) is required for macrophage maturation and growth [14], as CSF-1R–deficient mice have a considerably decreased number of macrophages [15]. We found that CSF-1R protein was reduced by 20%–25% in *Hri*$^{-/-}$ BMDMs on both day 3 and day 6, as shown by Western blot analysis (Figure 2D). Collectively, these results demonstrate that *Hri*$^{-/-}$ BMDMs are impaired in their maturation and that decreased CSF-1R expression is likely to be responsible for the impaired maturation.

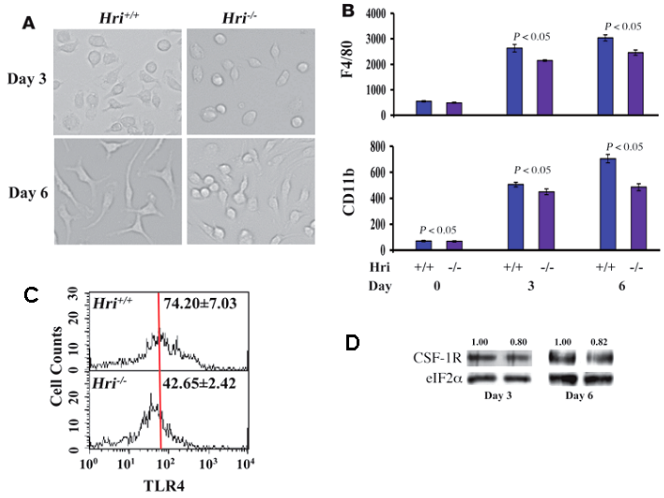

Figure 2. Impairment of macrophage maturation in *Hri*$^{-/-}$ BMDMs. (**A**) Cell morphology of *Hri*$^{+/+}$ and *Hri*$^{-/-}$ BMDM cultures. Original magnification, ×200. (**B**) FACS analyses of expression of macrophage surface markers F4/80 and CD11b. (**C**) FACS analyses of TLR4 protein expression at day 6. The peak intensity is shown in the upper-right corner of each diagram ($P < 0.01$). (**D**) Western blot analyses of CSF-1R protein expression at days 3 and 6. The ratios of CSF-1R to eIF2α are shown above the autoradiogram.

Role of HRI in iron recycling during chronic hemolytic anemia upon PHZ treatment. PHZ exposure induces hemolysis because it provokes denaturation of oxyhemoglobin, accumulation of Heinz bodies in erythrocytes, and damage of cells [16]. The damaged RBCs are mostly engulfed by macrophages in the spleen and liver. Recycling of iron from erythrophagocytosis by macrophages plays a critical role in erythropoiesis during chronic hemolytic anemia.

To investigate the potential role of HRI in erythrophagocytosis induced by PHZ, we examined erythrophagocytosis and iron homeostasis in a mouse model of a low dose of PHZ exposure. After PHZ treatment, both Hri$^{+/+}$ and Hri$^{-/-}$ mice developed a very mild anemia with increased reticulocyte counts (31.85% in Hri$^{+/+}$ and 53.29% in Hri$^{-/-}$ mice; $P < 0.001$) and splenomegaly (6-fold enlargement) but no significant decrease in hemoglobin content compared with control mice. These results demonstrated that the PHZ-induced chronic hemolytic anemia was well compensated in both Hri$^{+/+}$ and Hri$^{-/-}$ mice.

The hepatic hepcidin mRNA level was greatly decreased in PHZ-treated Hri$^{+/+}$ and Hri$^{-/-}$ mice ($P < 0.001$), in agreement with increased erythropoiesis. However, the hepcidin level in Hri$^{-/-}$ mice was lower than that in Hri$^{+/+}$ mice both with and without PHZ treatment ($P < 0.05$) (Figure 3A). As previously reported [17, 18], both hepatic and splenic non-heme iron content were increased after PHZ treatment (Figure 3B), consistent with the increased intestinal iron absorption in response to decreased hepcidin expression. However, these increases in iron content by PHZ treatment were significantly lower in Hri$^{-/-}$ mice. The hepatic and splenic iron concentrations in Hri+/+ mice were 18.7% and 20.5% lower, respectively (Figure 3B). Interestingly, serum iron was decreased after PHZ treatment in both Hri$^{+/+}$ and Hri$^{-/-}$ mice (Figure 3B), even though hepcidin expression was decreased. This is most likely attributable to the increased erythropoietic iron utilization. The slight increase in serum iron in PHZ-treated Hri$^{-/-}$ mice compared with PHZ-treated Hri$^{+/+}$ mice ($P < 0.05$; Figure 3B) may have been due to increased iron export by higher amounts of ferroportin protein as the result of lower hepcidin level in PHZ-treated Hri$^{-/-}$ mice (Figure 3A).

Importantly, non-heme iron staining of liver and spleen sections revealed that iron was present mainly in macrophages. Thus, the increase in non-heme iron in both spleen and liver were due to increased erythrophagocytosis of macrophages as the result of RBC damage by PHZ. As shown in Figure 4A, the difference in iron-laden macrophages between Hri$^{+/+}$ and Hri$^{-/-}$ mice was

most prominent in the liver. There was no visible iron staining in control livers. Livers from PHZ-treated mice exhibited iron staining only in the Kupffer cells and not in hepatocytes. Furthermore, ingested RBCs were visible in Kupffer cells (Figure 4A). We observed that PHZ-treated Hri$^{-/-}$ livers had 35.5% fewer iron-laden Kupffer cells (38.4 cells/field compared with 59.5 cells/field in Hri$^{+/+}$) and less iron per macrophage as indicated by the intensity of iron staining (Figure 4B).

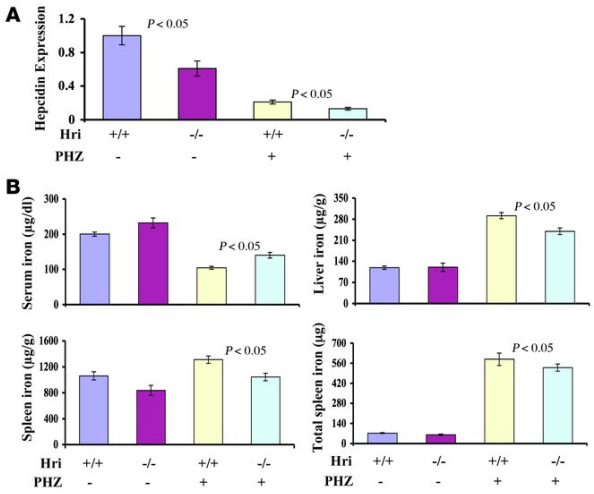

Figure 3. Hepatic hepcidin mRNA and tissue and serum iron content (**A**) Hepatic hepcidin mRNA expression before and after PHZ treatment. Hepcidin expression was significantly decreased after PHZ treatment in both *Hri*$^{+/+}$ and *Hri*$^{-/-}$ mice ($P < 0.05$), and its expression in *Hri*$^{-/-}$ mice was significantly lower than that in *Hri*$^{+/+}$ mice before and after PHZ treatment ($P < 0.05$). (**B**) Serum and tissue iron content before and after PHZ treatment. Results are presented as mean ± SEM ($n = 6–9$).

Together, these results demonstrate that increased iron in PHZ-induced hemolytic anemia is utilized entirely for erythropoiesis such that there is a decrease in serum iron and absence of iron accumulation in hepatocytes. Under this chronic hemolytic anemia condition, recycling of iron from senescent RBCs plays an important role in providing iron for erythropoiesis, as evidenced by iron-laden Kupffer cells in the liver and macrophages in the spleen. Lower iron contents in hepatic and splenic macrophages of PHZ-treated Hri$^{-/-}$ mice compared with PHZ-treated Hri+/+ mice indicate a decrease in erythrophagocytosis by Hri$^{-/-}$ macrophages in vivo. These results demonstrate that the deficiency of HRI in macrophages leads to the impairment of iron recycling in chronic hemolytic anemia.

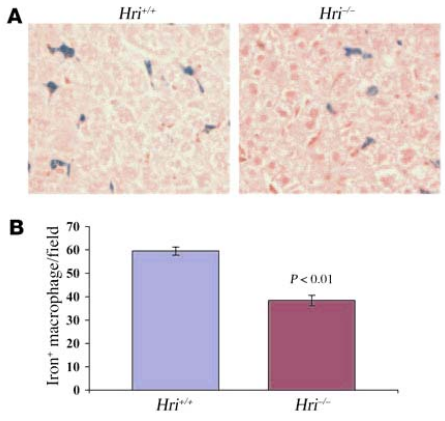

Figure 4. Impaired erythrophagocytosis by Kupffer cells in *Hri*$^{-/-}$ mice during chronic hemolytic anemia induced by PHZ. (**A**) Iron staining of liver tissue sections of *Hri*$^{+/+}$ and *Hri*$^{-/-}$ mice after PHZ treatment. (**B**) Numbers of iron-laden macrophages/field. The values represent the average number of iron-laden macrophages under a ×200 field ($n = 10$).

PHZ-treated *Hri*$^{-/-}$ mice exhibited impaired erythrophagocytosis by splenic and hepatic macrophages. The reduction in the increase of liver and spleen iron concentrations in *Hri*$^{-/-}$ mice upon PHZ treatment is consistent with the decreased erythrophagocytosis by *Hri*$^{-/-}$ macrophages. These findings provide evidence of the role of HRI in macrophages to recycle iron for erythropoiesis. In this regard, HRI also coordinates the supply of iron for hemoglobin synthesis in erythroid cells by recycling it from senescent RBCs under the stress conditions of hemolytic anemia.

In summary, the present study of chronic hemolytic anemia in *Hri*$^{-/-}$ mice reveals a novel function of HRI in macrophages and demonstrates the protective role of HRI with exposure to PHZ.

References:

1. Han, A.P., Yu, C., Lu, L., Fujiwara, Y., Browne, C., Chin, G., Fleming, M., Leboulch, P., Orkin, S.H., and Chen, J.J. (2001). Heme-regulated eIF2alpha kinase (HRI) is required for translational regulation and survival of erythroid precursors in iron deficiency. Embo J *20*, 6909-6918.
2. Han, A.P., Fleming, M.D., and Chen, J.J. (2005). Heme-regulated eIF2alpha kinase modifies the phenotypic severity of murine models of erythropoietic protoporphyria and beta-thalassemia. J Clin Invest *115*, 1562-1570.
3. Lu, L., Han, A.P., and Chen, J.J. (2001). Translation initiation control by heme-regulated eukaryotic initiation factor 2alpha kinase in erythroid cells under cytoplasmic stresses. Mol Cell Biol *21*, 7971-7980.
4. Nemeth, E., Tuttle, M.S., Powelson, J., Vaughn, M.B., Donovan, A., Ward, D.M., Ganz, T., and Kaplan, J. (2004). Hepcidin regulates cellular iron efflux by binding to ferroportin and inducing its internalization. Science *306*, 2090-2093.
5. Torrance, J.D., and Bothwell, T.H. (1980). Tissue iron stores. In Methods in hematology. J.D. Cook, editor. . Churchill Livingstone Press. New York, New York, USA., 104–109.
6. Delaby, C., Pilard, N., Goncalves, A.S., Beaumont, C., and Canonne-Hergaux, F. (2005). Presence of the iron exporter ferroportin at the plasma membrane of macrophages is enhanced by iron loading and down-regulated by hepcidin. Blood *106*, 3979-3984.
7. Vokurka, M., Krijt, J., Sulc, K., and Necas, E. (2006). Hepcidin mRNA levels in mouse liver respond to inhibition of erythropoiesis. Physiol Res *55*, 667-674.
8. Harding, H.P., Zhang, Y., Zeng, H., Novoa, I., Lu, P.D., Calfon, M., Sadri, N., Yun, C., Popko, B., Paules, R., Stojdl, D.F., Bell, J.C., Hettmann, T., Leiden, J.M., and Ron, D. (2003). An integrated stress response regulates amino acid metabolism and resistance to oxidative stress. Mol Cell *11*, 619-633.
9. Stout, R.D., and Suttles, J. (2005). Immunosenescence and macrophage functional plasticity: dysregulation of macrophage function by age-associated microenvironmental changes. Immunol Rev *205*, 60-71.
10. Ganz, T., and Nemeth, E. (2006). Regulation of iron acquisition and iron distribution in mammals. Biochim Biophys Acta *1763*, 690-699.
11. Andrews, N.C., and Schmidt, P.J. (2007). Iron homeostasis. Annu Rev Physiol *69*, 69-85.
12. Crosby, J.S., Lee, K., London, I.M., and Chen, J.J. (1994). Erythroid expression of the heme-regulated eIF-2 alpha kinase. Mol Cell Biol *14*, 3906-3914.
13. Akashi, S., Shimazu, R., Ogata, H., Nagai, Y., Takeda, K., Kimoto, M., and Miyake, K. (2000). Cutting edge: cell surface expression and lipopolysaccharide signaling via the toll-like receptor 4-MD-2 complex on mouse peritoneal macrophages. J Immunol *164*, 3471-3475.
14. Chitu, V., and Stanley, E.R. (2006). Colony-stimulating factor-1 in immunity and inflammation. Curr Opin Immunol *18*, 39-48.
15. Dai, X.M., Ryan, G.R., Hapel, A.J., Dominguez, M.G., Russell, R.G., Kapp, S., Sylvestre, V., and Stanley, E.R. (2002). Targeted disruption of the mouse colony-stimulating factor 1 receptor gene results in osteopetrosis, mononuclear phagocyte deficiency, increased primitive progenitor cell frequencies, and reproductive defects. Blood *99*, 111-120.
16. Itano, H.A., Hirota, K., and Hosokawa, K. (1975). Mechanism of induction of haemolytic anaemia by phenylhydrazine. Nature *256*, 665-667.
17. Ferrali, M., Signorini, C., Sugherini, L., Pompella, A., Lodovici, M., Caciotti, B., Ciccoli, L., and Comporti, M. (1997). Release of free, redox-active iron in the liver and DNA oxidative damage following phenylhydrazine intoxication. Biochem Pharmacol *53*, 1743-1751.
18. Frazer, D.M., Inglis, H.R., Wilkins, S.J., Millard, K.N., Steele, T.M., McLaren, G.D., McKie, A.T., Vulpe, C.D., and Anderson, G.J. (2004). Delayed hepcidin response explains the lag period in iron absorption following a stimulus to increase erythropoiesis. Gut *53*, 1509-1515.